bioRxiv preprint doi: https://doi.org/10.1101/398784; this version posted August 23, 2018. The copyright holder for this preprint (which was not certified by peer review) is the author/funder, who has granted bioRxiv a license to display the preprint in perpetuity. It is made available under aCC-BY-NC-ND 4.0 International license.

Tissue- and sex-specific small RNAomes reveal sex differences in response to the environment

Alexandra Bezler (alexandra.bezler@epfl.ch) [1, present address 2,3]
Fabian Braukmann (f.braukmann@gurdon.cam.ac.uk) [3,4,5,6]
Sean West (swest9@gmail.com) [7,8]
Arthur Duplan (arthur.duplan@hotmail.ch) [1]
Raffaella Conconi (raffaellaconconi@gmail.com) [1]
Frédéric Schütz (frederic.schutz@sib.swiss) [9]
Pierre Gönczy (pierre.gonczy@epfl.ch) [2]
Fabio Piano (fp1@nyu.edu) [7,10]
Kristin Gunsalus (kcg1@nyu.edu) [7,10]
Eric A. Miska (eam29@cam.ac.uk) [4,5,6,*]
Laurent Keller (laurent.keller@unil.ch) [1,*]

[1] Department of Ecology and Evolution, University of Lausanne, Switzerland
[2] Swiss Institute for Experimental Cancer Research (ISREC), School of Life Sciences, Swiss Federal Institute of Technology (EPFL), Lausanne, Switzerland
[3] These authors contributed equally to this work
[4] Gurdon Institute, University of Cambridge, Cambridge, UK
[5] Department of Genetics, University of Cambridge, Cambridge, UK
[6] Wellcome Sanger Institute, Wellcome Genome Campus, Cambridge, UK
[7] Center for Genomics & Systems Biology, Department of Biology, New York University, New York, NY
[8] Present address: Biologics Discovery California, Bristol-Myers Squibb, Redwood City, CA
[9] Bioinformatics Core Facility; SIB Swiss Institute of Bioinformatics and Centre for Integrative Genomics, University of Lausanne, Switzerland
[10] Center for Genomics & Systems Biology, NYU Abu Dhabi, Abu Dhabi, UAE

* Correspondence:

EAM (eam29@cam.ac.uk) and LK (laurent.keller@unil.ch).

KEYWORDS

germline sex, *C. elegans*, small RNA, RNA interference, RNA-seq

bioRxiv preprint doi: https://doi.org/10.1101/398784; this version posted August 23, 2018. The copyright holder for this preprint (which was not certified by peer review) is the author/funder, who has granted bioRxiv a license to display the preprint in perpetuity. It is made available under aCC-BY-NC-ND 4.0 International license.

ABSTRACT

Background

RNA interference (RNAi) related pathways are essential for germline development and fertility in metazoa and can contribute to inter- and trans-generational inheritance. In the nematode *Caenorhabditis elegans* environmental double-stranded RNA provided by feeding can lead to heritable changes in phenotype and gene expression. Notably, transmission efficiency differs between the male and female germline, yet the underlying mechanisms remain elusive.

Results

Here we use high-throughput sequencing of dissected gonads to quantify sex-specific endogenous piRNAs, miRNAs and siRNAs in the *C. elegans* germline and the somatic gonad. We identify genes with exceptionally high levels of 22G RNAs that are associated with low mRNA expression, a signature compatible with silencing. We further demonstrate that contrary to the hermaphrodite germline, the male germline, but not male soma, is resistant to environmental RNAi triggers provided by feeding. This sex-difference in silencing efficacy is associated with lower levels of gonadal RNAi amplification products. Moreover, this tissue- and sex-specific RNAi resistance is regulated by the germline, since mutant males with a feminized germline are RNAi sensitive.

Conclusion

This study provides important sex-and tissue-specific expression data of miRNA, piRNA and siRNA as well as mechanistic insights into sex-differences of gene regulation in response to environmental cues.

bioRxiv preprint doi: https://doi.org/10.1101/398784; this version posted August 23, 2018. The copyright holder for this preprint (which was not certified by peer review) is the author/funder, who has granted bioRxiv a license to display the preprint in perpetuity. It is made available under aCC-BY-NC-ND 4.0 International license.

BACKGROUND

The environment can induce changes in phenotype and gene expression that persist across multiple generations [reviewed in 1]. Such intra- and trans-generational inheritance can pass both through the male and female germlines. Several studies have revealed sex-differences in transmission efficiency of heritable phenotypic changes, yet the underlying molecular mechanisms remain unknown [2–5].

In the nematode *Caenorhabditis elegans,* environmental cues such as starvation, viral RNA or environmental RNA can trigger heritable phenotypic changes that are transmitted via small RNA [6–8]. The mechanisms of trans-generational inheritance are best understood from studies of environmental RNA [5,6,9–11]. In *C. elegans* phenotypic changes induced by environmental RNAi require a double stranded RNA (dsRNA) entering the animal via a dedicated dsRNA transporter [12,13]. Thereafter, exogenous dsRNAs are processed by the conserved nuclease Dicer into ~22 nucleotide (nt) primary small interfering RNAs (siRNA) and incorporated into Argonaute proteins to form the RNA-induced silencing complex (RISC) [14,15]. This protein-RNA complex binds complementary mRNA sequences and initiates the production of secondary siRNA by RNA-dependent RNA polymerases (RdRP) (Fig 1A) [16–18]. Such secondary siRNAs are 22 nt with a 5’ guanine, thus named 22G RNAs [19]. Primary and secondary siRNA trigger systemic gene silencing of complementary sequences through destabilization of mRNA or translational repression (Fig 1A)[20–22]. Once established, phenotypic

bioRxiv preprint doi: https://doi.org/10.1101/398784; this version posted August 23, 2018. The copyright holder for this preprint (which was not certified by peer review) is the author/funder, who has granted bioRxiv a license to display the preprint in perpetuity. It is made available under aCC-BY-NC-ND 4.0 International license.

84 changes induced by exogenous dsRNA can be transmitted over multiple
85 generations [9,11,22].
86
87 On top of their role in trans-generational inheritance, some endogenous small
88 RNA types – such as miRNA, piRNA and siRNA – are essential for
89 development and fertility in both sexes of *C. elegans*. Albeit distinguishable,
90 those small RNA types share some biogenesis and silencing mechanisms
91 (Fig 1A). One major class of small RNA, miRNAs, regulate translation of
92 mRNA targets via partially complementary base-pairing. Many miRNAs are
93 expressed in a tissue- and sex-specific specific manner reflecting functional
94 sex-differences [23–26]. For instance, miR-35 family activity in the female
95 germline is important for progeny viability and fecundity [27–29]. Furthermore,
96 distinct Argonaute proteins associate with additional types of endogenous
97 siRNAs in the male and female germline, suggesting functional sex-
98 differences [19,30–34]. Importantly, germline-expressed PIWI-bound
99 small RNA (piRNA) populations target mRNA and thus maintain genome
100 stability in hermaphrodites and males [35–38]. Such piRNAs come in two
101 flavours: type I piRNA are expressed from two genomic loci have a conserved
102 upstream motif, whereas type II piRNAs lack an apparent upstream motif and
103 are dispersed throughout the genome [39]. In *C. elegans,* another group of
104 endogenous small RNAs are expressed in the gonads of both sexes. Such
105 siRNAs can be distinguished by length and are either (i) primary products of
106 the RNAse III enzyme Dicer/DCR-1 (e.g., 26G RNA) or (ii) secondary
107 products of RNA-dependent RNA polymerases (e.g., 22G RNA) (Fig 1A).
108 Both types of endogenous siRNAs modulate gene expression and are

bioRxiv preprint doi: https://doi.org/10.1101/398784; this version posted August 23, 2018. The copyright holder for this preprint (which was not certified by peer review) is the author/funder, who has granted bioRxiv a license to display the preprint in perpetuity. It is made available under aCC-BY-NC-ND 4.0 International license.

essential for fertility, but very little is known about potential sex-differences in their gonadal expression [30,32,33].

The reproductive tissue of *C. elegans* consists of the germline surrounded by the somatic gonad, and development of both tissues is coordinated by multiple mechanisms [40]. Notably, miRNA activity in the somatic gonad is essential for gonad development and germline proliferation, and thus fertility [41,42]. However, a comprehensive tissue- and sex-specific expression study of gonadal siRNA is lacking.

Males and females also present germline sex-specific differences in response to environmental cues. First, RNAi in hermaphrodite gonads induces very strong knockdown phenotypes [2,43–45], in contrast to anecdotal evidence for mostly no detectable RNAi phenotypes in *C. elegans* sperm [2,43,46–48]. Second, siRNA induced trans-generational silencing is often more efficient through the female than the male germline [2–5]. The underlying mechanisms causing these sex-differences are not well understood.

Here we provide a comprehensive study of both the genetically-determined small RNAome and environmentally-induced siRNA silencing. First, we quantify sex-biased expression of miRNA, piRNA and siRNA in isolated male and female gonads. We further ascribe small RNA sex-differences to the germline or somatic gonad by comparing gonads of each sex to mutant male gonads (*fog-3*) with a female germline. Quantitative analysis of gonadal expression of mRNA and 22G RNA identified genes with low mRNA

bioRxiv preprint doi: https://doi.org/10.1101/398784; this version posted August 23, 2018. The copyright holder for this preprint (which was not certified by peer review) is the author/funder, who has granted bioRxiv a license to display the preprint in perpetuity. It is made available under aCC-BY-NC-ND 4.0 International license.

expression and high 22G RNA levels, a signature compatible with silencing. Second, using environmental RNAi targeting a GFP-sensor we show that germline RNAi silencing efficacy is determined by germline sex. This tissue-specific sex-difference in silencing efficacy was associated with lower levels of RNAi amplification products in male than female gonads. These data provide a mechanistic basis for sex-differences in germline RNAi efficacy with implications for trans-generational inheritance.

RESULTS

The small RNAome of male and hermaphrodite gonadal tissues

To identify small RNAs expressed in hermaphrodite and male gonads, we quantified small RNA populations (Fig 1A) from dissected *C. elegans* gonads by high-throughput sequencing (Fig 1B). This approach allowed us to simultaneously analyse and compare tissue-specific expression of miRNA, piRNA and siRNAs of *C. elegans* gonads.

miRNAs with sex-biased germline or somatic gonad expression

Of the 257 annotated miRNAs in the *C. elegans* genome (assembly WS235, miRBase release 21) we detected 93 in hermaphrodite gonads and 112 miRNAs in male gonads (Fig 1C; minimum 5 mean sense reads across replicates, additional file 2). To uncover quantitative differences in miRNA expression between sexes, we compared normalized read counts between hermaphrodite and male gonads. By using a cut-off of four-fold difference in abundance and a false-discovery rate of 1%, we identified 37 miRNAs with sex-biased gonad expression (Fig 1C).

bioRxiv preprint doi: https://doi.org/10.1101/398784; this version posted August 23, 2018. The copyright holder for this preprint (which was not certified by peer review) is the author/funder, who has granted bioRxiv a license to display the preprint in perpetuity. It is made available under aCC-BY-NC-ND 4.0 International license.

159 Since the gonads consist of two tissue types, the germline and the somatic
160 gonad, the observed difference between hermaphrodite and male may stem
161 from expression differences in either tissue. To determine the contribution of
162 the germline, we made use of mutant males that have a feminized germline
163 and a male somatic gonad (i.e., the loss of function allele *fog-3(q849[E126K]*
164 called *fog-3* or 'feminized male' for clarity) [49,50]. The comparison of the
165 control male and feminized male gonads allows one to uncover differences
166 that stem only from the germline, since both types of individuals have identical
167 male somatic gonads (Fig 1B). Of the 37 miRNAs with sex-biased gonad
168 expression, nine were differentially expressed between the male and
169 feminized male gonads (Fig 1D). Eight of them (including all form the miR-35-
170 41 cluster and miR-44) were expressed more highly in the feminized germline
171 (*fog-3* gonads) whereas only one (miR-8191) was more highly expressed in
172 the male germline (male gonads) (Fig 1D). This result shows for the first time
173 sex-specific expression of miRNAs in the *C. elegans* germline.
174
175 The comparison of hermaphrodite and feminized males permits to also
176 identify the contribution of the somatic gonad to differences in sex expression
177 between hermaphrodite and male gonads, since germlines are identical (both
178 female). This comparison revealed that 16 of the 37 miRNAs with sex-biased
179 gonad expression were differentially expressed between the hermaphrodite
180 and feminized gonads. One miRNA was more highly expressed in
181 hermaphrodites, and 15 miRNAs were more highly expressed in feminized
182 males, indicating sex-differences that stem from the somatic gonad (see
183 additional file 1 Fig S1).

bioRxiv preprint doi: https://doi.org/10.1101/398784; this version posted August 23, 2018. The copyright holder for this preprint (which was not certified by peer review) is the author/funder, who has granted bioRxiv a license to display the preprint in perpetuity. It is made available under aCC-BY-NC-ND 4.0 International license.

184 **piRNAs with sex-biased expression**

185 Next, we compared hermaphrodite and male gonads to identify type I and II
186 piRNAs with sex-biased expression. Our cloning technique allowed us to
187 capture (5'-monophosphate-) piRNAs, yet at lower frequency than other types
188 of (5'-triphosphate-) siRNA. We detected sense reads of 4004 annotated
189 piRNAs [36,51] in hermaphrodite gonads and 5390 in male gonads, including
190 3168 piRNAs present in both sexes (Fig 1E, additional file 2). To uncover
191 putative quantitative differences in piRNA expression between sexes, we
192 compared normalized read counts between hermaphrodite and male gonads.
193 Using a cutoff of four-fold difference in abundance and a false-discovery rate
194 of 1% revealed 66 piRNAs with hermaphrodite-biased expression and 919
195 piRNAs with male-biased expression (Fig 1F). piRNAs are germline specific,
196 and previous studies have identified male- and hermaphrodite-specific
197 piRNAs by sequencing of whole animals or purified gametes [36,37,52]. We
198 identified 93% of the previously identified male- and 32% of the female-biased
199 piRNAs in another study [52] despite differences between the two (i.e., cell
200 type, genotype, cloning technique and statistics). Thus, our method captures
201 differences in piRNA expression with more sex-specific piRNAs in males than
202 in hermaphrodites, further suggesting sex-specific regulatory mechanisms.
203
204 **Endogenous siRNAs with sex-biased germline expression**
205 As a third group of endogenous small RNA, we focused on siRNAs expressed
206 in gonads of both sexes. We analysed all siRNAs that map to protein coding
207 genes with a minimum of five mean antisense reads, thus excluding mRNA
208 degradation products with sense orientation. This revealed 8714 genes with

bioRxiv preprint doi: https://doi.org/10.1101/398784; this version posted August 23, 2018. The copyright holder for this preprint (which was not certified by peer review) is the author/funder, who has granted bioRxiv a license to display the preprint in perpetuity. It is made available under aCC-BY-NC-ND 4.0 International license.

siRNAs in hermaphrodite gonads and 10615 genes in male gonads (Fig 1G). 7675 of these siRNA targeted genes were found in both sexes (Fig 1G; additional file 2). Additional expression data of small RNA (antisense and sense) mapping to other annotated features in the genome such as pseudogenes, transposons and different types of small RNA for gonads of both sexes is available as additional file 2.

To detect potential quantitative expression differences between sexes, we compared normalized antisense read counts per gene between hermaphrodite and male gonads, selecting only genes with at least a four-fold difference in siRNA abundance and a false-discovery rate of 1%. 4508 genes exhibited a sex-biased expression of siRNAs: 1138 were higher expressed in hermaphrodites and 3370 were higher expressed in males. siRNAs of 68 genes were detected exclusively in hermaphrodites and 748 only in males.

To determine whether these expression differences stem from the germline or the somatic gonad, we again made use of the *fog-3* mutants. Of the 4508 genes with sex-biased siRNAs expression in the gonad, 3173 were also differentially expressed between the gonads of control males and feminized males. siRNAs mapping to 2245 genes were more highly expressed in the male gonads, and 928 were more highly expressed in the feminized male gonads (Fig 1H). Thus, most of the sex-differences between hermaphrodite and male gonads stem from expression differences in the germline proper.

bioRxiv preprint doi: https://doi.org/10.1101/398784; this version posted August 23, 2018. The copyright holder for this preprint (which was not certified by peer review) is the author/funder, who has granted bioRxiv a license to display the preprint in perpetuity. It is made available under aCC-BY-NC-ND 4.0 International license.

To relate sex-differences in germline siRNA expression to biological processes, we carried out gene set enrichment analysis using WormExp v1.0 [53]. This tool queries *C. elegans* mRNA and siRNA expression data in functional groups called 'gene sets' based on individual experiments for statistically significant overlap with a given gene list. We predicted that genes with sex-biased germline siRNA expression (i.e., 928 hermaphrodite- and 2245 male-biased genes) may overlap with gene sets corresponding to germline mRNA or siRNA expression. For statistical analysis, we compared enrichment to all 18106 genes with siRNAs detected. From the selected 912 gene sets queried (WormExp categories: mutants, tissue, other), there was significant overlap in both sexes with multiple gene sets related to germline mRNA expression (such as down-regulation in germline-less *glp-1* mutant; here and in the following comparisons $p<0.001$) and siRNA regulation (such as alteration in *csr-1*, *rde-1* and *rrf-3* mutants). In addition, this analysis revealed sex-specific overlap with several prior siRNA experiments. Genes with hermaphrodite-biased germline siRNA expression overlapped with siRNA targets detected in whole animals, for example those regulated by *rde-8*, *ergo-1*, *eri-6/-7*, *mut-16*. Likewise, genes with male-biased germline siRNA expression overlapped with spermatogenesis specific *alg-3/-4* targets. Thus, as expected, gonadal siRNAs with tissue-and sex-specific expression are involved in germline and siRNA functions, confirming the specificity of our approach.

High 22G RNA levels are associated with low mRNA expression, compatible with silencing

bioRxiv preprint doi: https://doi.org/10.1101/398784; this version posted August 23, 2018. The copyright holder for this preprint (which was not certified by peer review) is the author/funder, who has granted bioRxiv a license to display the preprint in perpetuity. It is made available under aCC-BY-NC-ND 4.0 International license.

Since 22G RNAs of several biogenesis pathways induce gene silencing, we determined the relative abundance of 22G RNAs in the gonads of both hermaphrodites and males. 22G RNAs represented 27.4% of reads in the hermaphrodite gonads and 27.9% of reads in the male gonads (additional file 1 Fig S2A). The 22G RNA levels per gene were not significantly different between the male (mean reads 234.4±1432.9) and hermaphrodite gonads (173.2±857.8; additional file 1 Fig S2B).

To gain insights into 22G RNA-mediated mRNA silencing in gonads, we tested if there was an association of 22G RNAs and corresponding mRNA template expression. If mRNA induces 22G RNA synthesis, there should be a positive correlation between the levels of mRNA and 22G RNA. Alternatively, if 22G RNA expression causes mRNA silencing, a negative correlation between the levels of mRNA and 22G RNA is expected. Data on gonadal mRNA expression in both *C. elegans* sexes was available from a previous study [54]. We first grouped genes in 20 bins according to their 22G RNA expression level. Across bins, there was a positive association between the levels of 22G RNA and gonadal mRNA for groups of genes with low and medium levels of 22G RNA (Fig 2). In contrast, in both hermaphrodites and males, the level of mRNA decreased with extremely high 22G RNA levels (Fig 2), a pattern suggestive of silencing. For statistical analyses we next grouped genes in 5% intervals with equal number of genes again according to 22G RNA expression (additional file 1 Fig S3A). The most significant negative association between the levels of 22G RNA and mRNA was found only for the 5% of the genes with highest level of 22G RNA expression (hermaphrodites

bioRxiv preprint doi: https://doi.org/10.1101/398784; this version posted August 23, 2018. The copyright holder for this preprint (which was not certified by peer review) is the author/funder, who has granted bioRxiv a license to display the preprint in perpetuity. It is made available under aCC-BY-NC-ND 4.0 International license.

283 $p=1x10^{-12}$, males $p=1x10^{-16}$; additional file 1 Fig S3B). These data indicate that
284 mRNA expression is globally decreased for genes with very high levels of
285 22G RNAs. In conclusion, the negative correlation of 22G RNA and mRNA
286 expression in *C. elegans* gonads is suggestive of siRNA mediated gene
287 silencing.
288
289 **Germline sex regulates environmental siRNA accumulation**
290 Since endogenous siRNA pathways share secondary siRNAs owing to similar
291 biogenesis routes [16,18,30], we cannot experimentally determine the fraction
292 of 22G RNA induced by a specific primary siRNA type. To compare
293 expression levels of both primary and secondary siRNA and their impact on
294 protein expression, we developed an sensor based assay. To this end, we
295 used a germline expressed GFP-sensor [55] targeted by *gfp(RNAi)*.
296 Environmental *gfp* dsRNA provided by feeding allows one to manipulate
297 primary siRNA levels and thus directly measure the impact of altered levels of
298 primary siRNA on secondary siRNA levels. To distinguish exogenous primary
299 siRNAs from worm-generated secondary siRNAs, we generated *gfp* dsRNA
300 with single-nucleotide-polymorphisms (SNPs) every 21 nucleotides relative to
301 the GFP-sensor transgene. Thus, primary siRNAs can be discriminated from
302 secondary siRNAs (Fig 3A). To investigate potential sex-specific regulation of
303 siRNA levels during exogenous RNAi, we quantified primary and secondary
304 siRNAs by sequencing siRNAs from gonads of males and hermaphrodites
305 expressing the GFP-sensor. Uptake and primary siRNA processing were
306 active in both male (9 siRNA/ 10^6 reads) and hermaphrodite gonads (6 siRNA/
307 10^6 reads). Moreover, primary siRNA levels were not statistically different

bioRxiv preprint doi: https://doi.org/10.1101/398784; this version posted August 23, 2018. The copyright holder for this preprint (which was not certified by peer review) is the author/funder, who has granted bioRxiv a license to display the preprint in perpetuity. It is made available under aCC-BY-NC-ND 4.0 International license.

between the sexes (t-test p=0.08, Fig 3B). By contrast, the secondary siRNA level was significantly lower in the male (82 siRNA/10^6 reads) than hermaphrodite gonads (280 siRNA/10^6 reads, t-test p=$4.3x10^{-3}$, Fig 3B). Accordingly, the ratio of secondary siRNA/ primary siRNA was significantly lower in the male gonads compared to the hermaphrodite gonads (respectively, 9 and 56 secondary siRNA/primary siRNA, t-test p=0.03, Fig 3B). Taken together, we conclude that environmental supplied dsRNA triggers primary and secondary siRNA production in the germline, with notably higher levels of secondary siRNA products in hermaphrodites than in males. The presence of primary siRNAs in the male germline establish that uptake and transport of silencing agents (such as dsRNA or primary siRNA) from the environment across male somatic tissues, notably the somatic gonad, is functional.

RNAi efficacy is germline sex dependent

Anecdotal evidence suggests that germline RNAi silencing may differ between *C. elegans* hermaphrodites and males. RNAi in hermaphrodite germlines is extremely potent as depletion phenotypes often appear within 24 hours of dsRNA exposure [45], even at reduced dsRNA dose [44]. In contrast, similar experiments generally provide negative RNAi results in male germlines [43,46,48]. Presumably stronger RNAi depletion occurs in male germlines directly injected with high doses of dsRNA [56], or by exposing the parental generation [57–60]. However, direct comparison of silencing efficacy of endogenous genes solely based on phenotypes in germlines of hermaphrodites and males is insufficient, notably due to sex differences in

bioRxiv preprint doi: https://doi.org/10.1101/398784; this version posted August 23, 2018. The copyright holder for this preprint (which was not certified by peer review) is the author/funder, who has granted bioRxiv a license to display the preprint in perpetuity. It is made available under aCC-BY-NC-ND 4.0 International license.

physiology and gene function. Feeding dsRNA triggers against the expressed GFP-sensor allows one to measure and compare siRNA levels and resulting RNAi silencing in hermaphrodites and males raised in the same environment. The observed difference in siRNA amplification products observed above (see Fig 3) prompted us to ask whether germline sex affects RNAi silencing. To assess RNAi silencing in both sexes, we monitored the presence or absence of GFP-sensor fluorescence upon *gfp(RNAi)* (Fig 4A). These analyses revealed that germline silencing by dsRNA is sex specific. Of the 307 hermaphrodites analysed, 305 (99.4%) silenced the germline GFP-sensor (Fig 4B), in contrast to only 3 (3.7%) of the 81 males analysed (chi-square $p<0.001$; Fig 4B). This difference pertained to the entire germline of males since GFP-sensor expression was visible in proliferating germ cells and differentiated spermatocytes (Fig 4A). Contrary to the germline, the soma of males was RNAi sensitive, as evidenced by the complete silencing of a ubiquitous GFP-sensor [61] in all non-neuronal somatic cells (Fig 4C; 60/60 males). This is in line with successful RNAi-based screens targeting somatic tissues in male, notably the somatic gonad [62,63] and shows that somatic RNAi efficacy is sex independent. Thus, isogenic worms raised in the same environment show phenotypic differences in response to environmental cues. Since RNAi silencing is dependent on the dsRNA levels and because mutants defective in siRNA amplification are partly RNAi resistant [16,64–66], the observed sex-difference in secondary siRNA abundance in gonads (Fig 3B) may explain the difference between sexes in germline RNAi efficacy (Fig 4A and 4B).

bioRxiv preprint doi: https://doi.org/10.1101/398784; this version posted August 23, 2018. The copyright holder for this preprint (which was not certified by peer review) is the author/funder, who has granted bioRxiv a license to display the preprint in perpetuity. It is made available under aCC-BY-NC-ND 4.0 International license.

358 **RNAi efficacy is germline sex dependent**

359 To determine whether the observed differences in germline RNAi silencing
360 between male and hermaphrodites was induced by differences in the germline
361 or the soma, we again made use of the feminized males. All other traits of the
362 feminized males such as soma, karyotype and feeding-behaviour are
363 undistinguishable from wild-type males (Fig 4B). Upon feeding *gfp(RNAi)*, all
364 106 feminized males silenced the GFP-sensor (Fig 4A, B), indicating that
365 germline-intrinsic factors regulate RNAi silencing, rather than other male traits
366 such as the soma, karyotype or behaviour.

367

368 To test whether differences in germline RNAi silencing between control and
369 feminized mutant male gonads could stem from altered siRNA levels or
370 altered downstream silencing activities, for instance target slicing by
371 Argonautes, we compared siRNA levels in gonads. The gonads of feminized
372 males contained higher levels of primary *gfp* siRNAs (74 siRNA/10^6 reads, t-
373 test $p=9.5x10^{-4}$) and secondary *gfp* siRNAs (798 siRNA/10^6 reads, t-test
374 p=0.04) than control male gonads (additional file Figure S4). Since RNAi
375 silencing is dose-dependent, the higher siRNA levels in feminized mutant
376 compared to male gonads are a plausible explanation for the sex-difference in
377 germline RNAi silencing.

378

379 To examine whether the male germline RNAi resistance was inherent to
380 sperm or influenced by the surrounding germline environment, we compared
381 RNAi silencing between the sperm of males and hermaphrodites. If the
382 germline environment regulates RNAi, silencing should differ between the

bioRxiv preprint doi: https://doi.org/10.1101/398784; this version posted August 23, 2018. The copyright holder for this preprint (which was not certified by peer review) is the author/funder, who has granted bioRxiv a license to display the preprint in perpetuity. It is made available under aCC-BY-NC-ND 4.0 International license.

sperm of males and hermaphrodites. By contrast, if the sperm physiology confers RNAi resistance, both types of sperm should be RNAi resistant. We measured fluorescence intensities of a GFP-sensor [67] on chromatin using both types of sperm imaged in whole worms fed with *gfp(RNAi)*. This experiment revealed RNAi silencing in hermaphrodite sperm, since *gfp(RNAi)* significantly decreased sperm GFP signal intensity by a mean of 81.9%±5.1% compared to animals not exposed to dsRNA (Fig 4D; t-test $p=1.8x10^{-6}$). By contrast, the sperm of males was completely RNAi resistant, with the GFP-sensor signal intensity being not significantly different between males fed with *gfp(RNAi)* and males not being exposed to dsRNA (Fig 4D; t-test p=0.2).

The finding that, in contrast to sperm in males, sperm from hermaphrodites is RNAi sensitive, indicates that the surrounding germline environment plays a crucial role in RNAi silencing of sperm. Because germ cell precursors for sperm and oocytes grow in the same syncytium in hermaphrodites, silencing agents such as siRNAs or RNAi proteins produced in oocytes may diffuse in the germline and thus influence silencing in sperm. To test this hypothesis, we investigated whether mutant hermaphrodites producing only sperm initiate RNAi independently of oogenic germ cells using the gain-of-function allele *fem-3(q96)* [68]. We found that such sperm were RNAi sensitive, since fluorescence GFP-sensor [67] signal intensity was on average 74.8%±19.9% lower in *fem-3* worms fed *gfp(RNAi)* compared to animals not exposed to RNAi (Fig 4D; t-test $p=3.0x10^{-7}$). Thus, the sperm of hermaphrodites is RNAi sensitive even in the complete absence of oogenic germ cells in the syncytium.

bioRxiv preprint doi: https://doi.org/10.1101/398784; this version posted August 23, 2018. The copyright holder for this preprint (which was not certified by peer review) is the author/funder, who has granted bioRxiv a license to display the preprint in perpetuity. It is made available under aCC-BY-NC-ND 4.0 International license.

DISCUSSION

Here we provide the first comprehensive small RNA profile of isolated *C. elegans* male and hermaphrodite gonads and show qualitative as well as quantitative sex-differences in siRNA expression for both somatic gonad and germline tissue. We demonstrate tissue-specific sex-differences in response to environmental RNAi triggers: in contrast to the hermaphrodite germline, the male germline is resistant to silencing and accumulates lower levels of RNAi amplification products. Taken together, these results provide a mechanistic explanation for sex-differences in RNAi efficacy in response to the environment with implications for trans-generational inheritance.

Sex-differences in gonadal miRNA, piRNA and siRNA expression

miRNA regulation, notably via the conserved miR-35 family is crucial for the embryonic viability, proliferation of the germline and is implicated in sex-determination [27,28,41,69]. In addition, miRNAs expressed in the *C. elegans* somatic gonad maintain germline proliferation and differentiation [41]. We identified female germline-biased expression of the miR35-41 cluster in isolated gonads, which is in line with studies conducted on whole animals [27,29,70].

The transgene reporter for miR-246 expression, which typically escapes germline expression, was previously observed in hermaphrodite gonadal sheath cells [23]. Here we establish sex-biased expression of endogenous miR-246 specifically in the hermaphrodite somatic gonad as opposed to the

bioRxiv preprint doi: https://doi.org/10.1101/398784; this version posted August 23, 2018. The copyright holder for this preprint (which was not certified by peer review) is the author/funder, who has granted bioRxiv a license to display the preprint in perpetuity. It is made available under aCC-BY-NC-ND 4.0 International license.

433 germline or the male gonad. Since miR-246 expression positively correlates
434 with lifespan [71,72], it will be interesting to identify miR-246 targets in the
435 somatic gonad or germline. Thus, small RNA sequencing of isolated gonads
436 and comparison of expression differences between wild-type and sex-
437 transformed mutant gonads captures known sex-differences in expression
438 and in addition provides more detailed, tissue-specific information.
439
440 Our data provide the first tissue-specific analysis of miRNA expression in
441 males. Of the 46 male-biased miRNAs with searchable names in miRBase
442 detected in whole animals [24], 13 miRNAs showed male-biased gonad
443 expression, underlining the importance of a tissue-specific approach. Thus,
444 sex-biased miRNA expression occurs in both soma and gonad. Some
445 miRNAs with male-biased gonad expression were previously not detected as
446 sex-biased [24] and could have been masked by somatic expression in both
447 sexes.
448
449 In contrast to miRNAs, the piRNA pathway acts exclusively in the germline.
450 Since the germline makes up about half of the adult *C. elegans* cells [73],
451 whole worm sequencing is a good proxy for germline-restricted piRNA
452 expression. Our analysis of sex-biased piRNA expression thus complements
453 previous studies on whole animals that reported distinct piRNA expression in
454 hermaphrodites and males [24,37]. While the cloning method applied here
455 causes relatively low (5'-monophasphate) piRNA detection level compared to
456 whole animals [37], it also causes preferential cloning of 5'-triphosphate RNA
457 species and thus high coverage of endogenous siRNA. The tissue-specific

bioRxiv preprint doi: https://doi.org/10.1101/398784; this version posted August 23, 2018. The copyright holder for this preprint (which was not certified by peer review) is the author/funder, who has granted bioRxiv a license to display the preprint in perpetuity. It is made available under aCC-BY-NC-ND 4.0 International license.

458 analysis of endogenous 22G RNA and mRNA identified transcripts that are
459 potentially regulated by RNAi. Importantly, hermaphrodites and males share
460 common as well as distinct siRNA targeted gene sets in gonadal tissue. Most
461 gonadal sex-differences in siRNA expression stem from the germline, which
462 represents the vast majority of the gonadal tissue. Further comparison of
463 gonadal siRNA and corresponding mRNA uncovers uncoupling of siRNA and
464 mRNA levels, indicative of RNAi silencing. It will be interesting to investigate
465 this regulation in the future.
466
467 **RNAi efficacy is regulated by germline sex**
468 Our study provides novel insights into how the sex of an animal influences
469 RNA-induced environmental changes in the phenotype. In particular, using
470 environmental dsRNA triggers, we demonstrated that RNAi resistance affects
471 exclusively the male germline. Sequencing primary and secondary siRNA with
472 unique SNPs in isolated gonads from males and hermaphrodites allowed us
473 to quantitatively compare steady-state levels. We detected similar levels of
474 primary siRNAs in gonads of both sexes, suggesting functional transport of
475 RNAi trigger from the environment to the soma and processing of primary
476 siRNA in the male germline. In contrast, we discovered low levels of
477 secondary siRNA amplification products in males compared to
478 hermaphrodites. Thus, RNAi resistance in the male germline affects
479 downstream processes that likely impact sex-differences in secondary siRNA
480 processing or siRNA stability. It follows that RNAi is generally not suitable for
481 functional studies of the *C. elegans* male germline if provided during one

bioRxiv preprint doi: https://doi.org/10.1101/398784; this version posted August 23, 2018. The copyright holder for this preprint (which was not certified by peer review) is the author/funder, who has granted bioRxiv a license to display the preprint in perpetuity. It is made available under aCC-BY-NC-ND 4.0 International license.

generation only. Since RNAi silencing is efficient in sperm of hermaphrodites, such animals are more suitable for reverse genetics targeting the germline.

What determines the sex-differences of gene regulation in response to environmental cues? It is conceivable that known or novel RNAi regulators impact germline gene regulation by modulating RNAi efficacy. A potential candidate is the endoribonuclease RDE-8 which is expressed predominantly in hermaphrodite germlines and is essential for amplification of siRNA products and silencing [66]. Thus, RNAi resistance in male germlines may possibly be linked to reduced RDE-8 activity. Also, sex-differences in localization may affect RNAi efficacy. Notably CID-1, a poly(U)-polymerase modulating germline RNAi efficacy shows distinct subcellular localization in male and female germlines – perinuclear, respectively chromosomal- that may affect function [74]. Intriguingly, in addition, multiple sex-differences are well described for the Argonaute CSR-1 that targets endogenous germline transcripts via secondary 22G RNAs [19,34]. First, males and hermaphrodites express distinct CSR-1 isoforms [34,73]. Second, *csr-1* mutant hermaphrodites are mostly sterile, while *csr-1* mutant males show only modestly reduced fertility over multiple generations [33,75]. Third, CSR-1 bound 22G RNAs target distinct sets of transcripts in male and hermaphrodite [33,75]. Thus, sex-differences in CSR-1 function may contribute to the observed sex-difference in RNAi sensitivity, in line with CSR-1 function in germline RNAi [76]. Overall, multiple mechanisms may contribute to sex-specific gene regulation and untangling the individual contributions will provide exiting answers on male and female biology.

bioRxiv preprint doi: https://doi.org/10.1101/398784; this version posted August 23, 2018. The copyright holder for this preprint (which was not certified by peer review) is the author/funder, who has granted bioRxiv a license to display the preprint in perpetuity. It is made available under aCC-BY-NC-ND 4.0 International license.

In conclusion, this study provides the tissue-specific small RNAome of *C. elegans* hermaphrodite and male gonads and identifies quantitative sex-differences in miRNA, piRNA and siRNA expression. Furthermore, we demonstrate that the male germline is resistant to RNAi triggers taken up from the environment and accumulates lower levels of RNAi amplification products. We thus provide mechanistic insights into sex-differences of gene regulation in response to environmental cues that may play a role in transgenerational inheritance.

MATERIAL AND METHODS

Nematode strains

C. elegans strains of the following genotype were cultured according to standard procedures [77]: *him-8(e1489)* IV [77], *fog-3(q849[E126K])* I/ hT2*[qIs48]* (I;III); (kind gift from Scott Aoki and Judith Kimble) and *fem-3(q96)* IV [68]. The following GFP-sensors were used: single copy *mjIs145* [mex-5p::GFP::his-58::21UR-1sense::tbb-2 3'UTR] II (Bagijn 2012; Figure 1, 2, 3, 4A, B), multicopy *adIs2122* [lgg-1p::GFP::lgg-1 *3'UTR* + rol-6(su1006)] [61]; Figure 4C) and multicopy *zuIs178* [*his-72p::his-72::GFP:his-72 3'UTR*] ([67]; Figure 4D). All strains were wild-type for *mut-16(mg461)* by PCR [78]. *him-8(e1489)* was used to generate otherwise wild-type males and hermaphrodites, for simplicity we refer to such animals as 'control males' and 'control hermaphrodites'.

RNA interference

bioRxiv preprint doi: https://doi.org/10.1101/398784; this version posted August 23, 2018. The copyright holder for this preprint (which was not certified by peer review) is the author/funder, who has granted bioRxiv a license to display the preprint in perpetuity. It is made available under aCC-BY-NC-ND 4.0 International license.

RNAi feeding plates where prepared from freshly streaked HT115 bacteria containing L4440 vector according to [79]. Those were used to feed synchronized L1 worms minimum 48h at 20°C unless otherwise stated. Initial *gfp(RNAi)* experiments were carried out with a construct targeting the full *gfp* coding sequence including three introns. The recoded *gfp(RNAi)* with SNP every 21 nucleotides targets only exons and was synthesized by Integrated DNA Technologies and cloned into the L4440 plasmid. Silencing efficiency of recoded *gfp(RNAi)* is slightly reduced compared to full length *gfp(RNAi)*, which may be caused by SNPs or lacking exons.

Microscopy

RNAi silencing was scored in live adults mounted on slides with reaction wells (Paul Marienfeld) using 20x or 40x objective on a Zeiss Axio Scope.A1 microscope. Worms scored as RNAi sensitive on a binary scale if GFP-sensor was absent or greatly diminished as compared to animals treated with empty vector RNAi. Differential interference contrast (DIC) and fluorescence images were acquired on a Axiocam 506 mono CCD camera and processed with Fiji software [80]. Outlines of the germlines where drawn on the DIC image in Adobe Illustrator.

Gonad isolation and replicates

Bleach-synchronized L1 worms were grown on RNAi bacteria 48h at 20°C until L4/ young adult, then washed 5 times in 15mL M9 to remove bacteria and grown overnight at 20°C on OP50 bacteria. Prior dissection, adults were picked on empty plates and transferred in groups of 3-4 in a drop of 0.01%

bioRxiv preprint doi: https://doi.org/10.1101/398784; this version posted August 23, 2018. The copyright holder for this preprint (which was not certified by peer review) is the author/funder, who has granted bioRxiv a license to display the preprint in perpetuity. It is made available under aCC-BY-NC-ND 4.0 International license.

557 levamisole + sperm buffer [81] to wash and paralyze animals. Animals were
558 cut with a 21G needle behind the pharynx to liberate the gonad in a new drop
559 of buffer on a depression slide (cavity 15-18mm, depth 0.6-0.8 mm;
560 Marienfeld). Non-gonadal somatic tissue was removed, including the intestine;
561 the spermatheca was removed from hermaphrodite gonads. Using a mouth
562 pipette with glass capillary gonads where transferred to a tube with RNAlater
563 (50-100µl) and after TRIzol (Thermo Fisher) addition frozen at -80°C.
564
565 Gonads from hermphrodites (100), males or *fog-3* males (each 200) were
566 processed as independent replicates for sequencing as follows (# replicates;
567 including # recoded *gfp(RNAi)* samples): hermaphrodites (6;4), males (3;2)
568 and *fog-3* males (2;2). Since endogenous siRNAs levels were not different
569 from germlines treated with or without *gfp(RNAi)*, both were used for sex-
570 biased expression analysis.
571
572 **RNA extraction**
573 RNA was extracted with 1 ml of TRIzol according to manufactor's protocol.
574 Briefly, RNA was precipitated adding 1 volume of isopropanol and 20 µg
575 glycogen (Roche). Samples forming a white precipitate at this point were
576 cleared by addition of 500 µL isopropanol: water 50 % (v/v). Samples were
577 frozen at -80°C, thawed on ice and RNA was pelleted by centrifugation for 30
578 min at +4°C, 16000 g. The pellet was washed in ice cold 70% (v/v) ethanol
579 and recovered by centrifugation for 20 min at +4°C, 16000 g and finally
580 resuspended in 10 µL water. RNA concentration was determined by Qubit®
581 RNA BR Assay Kit (Thermo Fisher).

bioRxiv preprint doi: https://doi.org/10.1101/398784; this version posted August 23, 2018. The copyright holder for this preprint (which was not certified by peer review) is the author/funder, who has granted bioRxiv a license to display the preprint in perpetuity. It is made available under aCC-BY-NC-ND 4.0 International license.

582

583 **5' independent library preparation and sequencing**

584 For RNA dephosphorylation 400 ng of RNA were treated with 20 Units of 5'
585 polyphosphatase (Epicenter) in 20 µL reaction volume, purified using acid-
586 phenol-chloroform, pH 4.5 (Thermo Fisher) and isopropanol precipitated using
587 20 µg of glycogen. Subsequently, RNA was suspended in 6 µL water and
588 directly used for TruSeq Small RNA library kit (Illumina) following the
589 manufacturer's instructions with exception that 15 cycles of PCR amplification
590 were used. The cDNA libraries were separated on 6% TBE PAGE gels (Life
591 Technologies) and bands with 147- 157 nucleotides were cut from the gel.
592 The gel matrix was broken by centrifugation through gel breaker tubes (IST
593 Engineering Inc.) and size-selected cDNA eluted with 400 µl of 0.3M Na-
594 Chloride. cDNA was purified by centrifugation through Spin-X 0.22µm
595 cellulose acetate filter columns (Costar) followed by isopropanol precipitation.
596 Libraries were sequenced on a HiSeq 1500 Sequencer (Illumina).

597

598 **Computational analysis of small RNA high-throughput sequencing data**

599 Small RNA sequencing results were obtained from
600 https://basespace.illumina.com/ as fastq files after demultiplexing. Sequencing
601 data is available in the European Nucleotide Archive under accession number
602 PRJEB12010. Firstly, adapter sequences, reads shorten than 21 nucleotides
603 (nt) and reads longer than 34 nt were removed using cutadapt v1.9.1.
604 Secondly, the remaining reads were aligned using bowtie 1.1.2 with at most 2
605 mismatches to *Escherichia coli* str. K-12 MG1655. Thirdly, the remaining
606 reads were aligned with at most 2 mismatches to *C. elegans* WS235 tRNAs

bioRxiv preprint doi: https://doi.org/10.1101/398784; this version posted August 23, 2018. The copyright holder for this preprint (which was not certified by peer review) is the author/funder, who has granted bioRxiv a license to display the preprint in perpetuity. It is made available under aCC-BY-NC-ND 4.0 International license.

and rRNAs. Fourthly, the remaining reads were aligned with no mismatches to the worm *gfp* sequence. Fifthly, the remaining reads were aligned with no mismatches to the recoded *gfp* sequence. Sixthly, the remaining reads were aligned with no mismatches to *C. elegans* miRNAshairpins (miR-base release 21). Seventhly, the remaining reads were aligned with no mismatches to *C. elegans* genome cel235. Overall, we obtained ~2.3 – 12.8 million trimmed reads mapping to the genome (WS235) for each sex. endo-siRNAs was quantified per gene, antisense reads mapping to coding exons, which account for more than 96% of reads in this class.

Silencing of mRNA targeted by very high levels of 22G RNA:

Fastq-mcf (Erik Aronesty (2011). ea-utils : "Command-line tools for processing biological sequencing data"; https://github.com/ExpressionAnalysis/ea-utils) was used to trim adapters from single-end reads. Bowtie 1.1.2 (parameters “--best --strata --tryhard -m 1”) (Langmead B, Trapnell C, Pop M, Salzberg SL. Ultrafast and memory-efficient alignment of short DNA sequences to the human genome. *Genome Biol* 10:R25.) was used to map single-ended reads to *C. elegans* WS250 genome. Reads were classified as 22G/26G based on length and starting base. HTSeq 0.6.0 (Simon Anders, Paul Theodor Pyl, Wolfgang Huber *HTSeq — A Python framework to work with high-throughput sequencing data* Bioinformatics 2014) was used to generate counts for reads that map to WS250 features in the sense and antisense directions. Reads mapping against transposons were retrieved using c_elegans.PRJNA13758.WS250.annotations.exons.genes.with_transposons.

bioRxiv preprint doi: https://doi.org/10.1101/398784; this version posted August 23, 2018. The copyright holder for this preprint (which was not certified by peer review) is the author/funder, who has granted bioRxiv a license to display the preprint in perpetuity. It is made available under aCC-BY-NC-ND 4.0 International license.

gff. Features counts from separate samples were normalized and differences in expression were determined using DESeq2 1.13.8 (Love MI, Huber W and Anders S (2014). "Moderated estimation of fold change and dispersion for RNA-seq data with DESeq2). Because alternative biological processes generate sense and antisense mapping reads, reads mapping in the sense direction from each library were normalized together, likewise reads mapping in the antisense direction were separately normalized. The cutoff for sex-biased expression was >4 fold difference in abundance and adjusted p-value <0.01. For correlations with germline transcriptome, data was used from West et al., Genome Biology 2017 (Sequence Read Archive, accession number SRP096640). For miRNAs both star and non-star sequences from the same gene were summed.

Assay and quantification of primary and secondary *gfp* siRNA levels: Reads were trimmed with cutadapt v1.9.1. Bacteria, tRNA and rRNA reads contaminations were removed using bowtie 1.1.2 alignment to the *Escherichia coli* str. K-12 MG1655 and to *C. elegans* WS235 tRNAs and rRNAs. Remaining reads were aligned with no mismatches to the worm *gfp* sequence. Then the remaining reads were aligned with no mismatches to the recoded *gfp* sequence.

LIST OF ABBREVIATIONS

RNA interference (RNAi)

Nucleotide (nt)

RNA-induced silencing complex (RISC)

bioRxiv preprint doi: https://doi.org/10.1101/398784; this version posted August 23, 2018. The copyright holder for this preprint (which was not certified by peer review) is the author/funder, who has granted bioRxiv a license to display the preprint in perpetuity. It is made available under aCC-BY-NC-ND 4.0 International license.

RNA-dependent RNA polymerases (RdRP)

PIWI bound small RNA (piRNA)

Green fluorescent protein (gfp)

Single-nucleotide-polymorphism (SNP)

DECLARATIONS

Ethics approval and consent to participate

Not applicable.

Consent for publication

Not applicable.

Availability of data and material

Small RNA library sequencing data is available on the European Nucleotide Archive in the Study: PRJEB12010. A sample description can be found in additional file 3.

Competing interests

The authors declare that they have no competing interests.

Funding

This work was funded by grants from the Swiss NSF and an advanced ERC grant to LK, grants from Cancer Research UK (C13474/A18583, C6946/A14492) and the Wellcome Trust (104640/Z/14/Z, 092096/Z/10/Z) to EAM, and grants from the National Institutes of Health to SW (NIGMS NHRA 5F32GM100614) and to FP and KCG (NHGRI U01 HG004276, NICHD R01 HD046236), and by research funding from New York University Abu Dhabi to FP and KCG.

bioRxiv preprint doi: https://doi.org/10.1101/398784; this version posted August 23, 2018. The copyright holder for this preprint (which was not certified by peer review) is the author/funder, who has granted bioRxiv a license to display the preprint in perpetuity. It is made available under aCC-BY-NC-ND 4.0 International license.

Authors' contributions

AB and FB contributed equally to experimental design, collected data, analysed and interpreted results, and drafted the manuscript. SW contributed to analysis design and interpretation of data and results. RC and AD contributed to cloning and data collection with GFP-sensor strains. FS provided statistical analysis for Fig 2. PG, KG and FP were involved in the conception and design of experiments and analyses. LK and EAM contributed to design of experiments and analyses, results interpretation and drafting the manuscript. All authors read and approved the final manuscript

Acknowledgements

We are grateful to Scott Aoki and Judith Kimble for sharing strains prior to publication, Benita Wolf, Adria LeBoeuf and Tamara Mikeladze-Dvali for comments on the manuscript and Gönczy lab members for advice. We thank Kay Harnish of the Gurdon Institute Sequencing Facility for managing the high-throughput sequencing, Nazife Bega for media preparation and Wormbase. Some strains were provided by the CGC, which is funded by NIH Office of Research Infrastructure Programs (P40 OD010440).

FIGURE LEGENDS

Figure 1: Tissue- and sex-specific small RNA profiling

A) Small RNA types in *C. elegans* categorized by template (DNA or RNA), length and first nucleotide (nt). Distinct primary small RNA types (orange) induce the amplification of secondary 22G RNAs (green) by RNA-dependent RNA polymerase (RdRP) using mRNA as a template.

bioRxiv preprint doi: https://doi.org/10.1101/398784; this version posted August 23, 2018. The copyright holder for this preprint (which was not certified by peer review) is the author/funder, who has granted bioRxiv a license to display the preprint in perpetuity. It is made available under aCC-BY-NC-ND 4.0 International license.

B) Small RNAs were sequenced from dissected adult *C. elegans* gonads containing germline and somatic gonad tissue. Control hermaphrodites and males have sex-specific germline and somatic gonad tissue (red: female traits; blue: male traits). Mutant *fog-3* males have a 'female' germline (red) and a male somatic gonad (blue).

C,E,G) Gonad expression of miRNA (C), piRNA (E) and endogenous siRNA (G, >5 mean reads) in control hermaphrodites (red circle, n=6 replicates) and males (blue circle n=3). Total number of gonadal small RNAs in each sex is shown as well as the overlap.

D,F,H) Sex-differences in expression of mean normalized miRNA (D), piRNA (F) and endogenous siRNA (H) reads in hermaphrodite (n=6 replicates) and male gonads (n=3). (D,H) miRNA and siRNA expression-differences with four-fold difference in abundance that were statistically different (Wilcoxon rank sum test with continuity correction; p adjusted<0.01) between hermaphrodites and males as well as between control males and *fog-3* males (n=2) are highlighted in red (female germline-biased) and blue (male germline-biased). (F) Since piRNA are germline-specific, expression-differences between hermaphrodites and males (n=2) are highlighted in red (female germline-biased) and blue (male germline-biased) without comparison to *fog-3*. See additional file 1 Fig S1 for sex-differences in somatic gonad expression.

Figure 2: High 22G RNA levels are associated with low mRNA expression, compatible with silencing

bioRxiv preprint doi: https://doi.org/10.1101/398784; this version posted August 23, 2018. The copyright holder for this preprint (which was not certified by peer review) is the author/funder, who has granted bioRxiv a license to display the preprint in perpetuity. It is made available under aCC-BY-NC-ND 4.0 International license.

Mean normalized mRNA [54] and 22G RNA reads detected in hermaphrodite and male gonads (data in 20 bins according to 22G RNA level; number of genes per bin: 4 – 1101 in hermaphrodites, 5 – 1343 in males; mean: solid line, outliers: open circles). mRNA expression is globally decreased for the top 5% of genes (shaded area) with high levels of 22G RNA. See additional file Fig S3 for statistical analysis.

Figure 3: Sex-differences in gonadal siRNA levels during germline RNAi silencing.

A) Assay to quantify primary and secondary siRNA levels (from dissected gonads from hermaphrodites and males; see Fig 1B). Animals expressing the GFP-sensor in the germline were raised on *gfp(RNAi)* containing SNPs (black square) each 21 nucleotides. Primary siRNAs (orange) are identified by the presence of the SNPs, while secondary siRNAs (green) lack SNPs.

B) Mean primary and secondary siRNA reads normalized to total reads in gonads from hermaphrodites (circles indicate replicates, n=4) and males (n=2). Animals raised on *gfp(RNAi)* or control empty vector (hermaphrodite n=2, male n=1). Mean secondary siRNA/ primary siRNA ratio only shown for RNAi treated animals. T-test was applied for significance test; * = $p<0.05$, *** = $p<0.001$.

Figure 4: Sex-differences in germline RNAi efficacy.

bioRxiv preprint doi: https://doi.org/10.1101/398784; this version posted August 23, 2018. The copyright holder for this preprint (which was not certified by peer review) is the author/funder, who has granted bioRxiv a license to display the preprint in perpetuity. It is made available under aCC-BY-NC-ND 4.0 International license.

A) Fluorescence microscopy images of germline (dotted line) GFP-sensor expression in hermaphrodites, males and *fog-3* males (left). Silencing of the GFP-sensor upon *gfp(RNAi)* in hermaphrodite and *fog-3* male germlines, while control male germlines are RNAi resistant (right). Gut autofluorescence is visible outside the germline.

B) Percentage of worms (±SEM) silencing the GFP-sensor in the germline upon *gfp(RNAi)* (n=307 hermaphrodites, 81 males, 106 *fog-3* males). Chi-square test was applied; *** = p<0.001. Table with hermaphrodite/ female (red) and male (blue) traits in hermaphrodites, males and *fog-3* males.

C) Fluorescence microscopy images of ubiquitous GFP-sensor expression in the soma of hermaphrodites and males (left, for both n=54). *gfp(RNAi)* silencing of somatic GFP in non-neuronal cells was observed in all hermaphrodites and males (right, respectively n=57 and n= 60).

D) Background subtracted sperm GFP-sensor chromatin signal intensity (mean ±SE) upon *gfp(RNAi)* in hermaphrodites (n=10), males (n=9) and *fem-3* hermaphrodites producing only sperm (n=15). Signal intensity was normalized to animals not exposed to dsRNA (n=10 hermaphrodites, 11 males, 12 *fem-3* hermaphrodites). T-test was applied for significance test; *** = p<0.001.

ADDITIONAL DATA

Additional file 1.pdf: Supplemental figures S1-S4.

SUPPLEMENTAL FIGURE LEGENDS

bioRxiv preprint doi: https://doi.org/10.1101/398784; this version posted August 23, 2018. The copyright holder for this preprint (which was not certified by peer review) is the author/funder, who has granted bioRxiv a license to display the preprint in perpetuity. It is made available under aCC-BY-NC-ND 4.0 International license.

Figure S1: Somatic gonad sex-differences in expression of miRNA and endogenous siRNA.

A) Mean normalized miRNA reads (sense) in hermaphrodite (n=6 replicates) and male gonads (n=3). miRNA expression-differences with four-fold difference in abundance that were statistically different (Wilcoxon rank sum test with continuity correction; p adjusted<0.01) between gonads of hermaphrodites and males as well as between hermaphrodites and *fog-3* males (n=2) are highlighted in red (female somatic gonad-biased) and blue (male somatic gonad-biased).

B) Mean normalized endogenous siRNA reads (antisense) in hermaphrodite and male gonads; same analyses and representation used as in Fig S1A.

Figure S2: Hermaphrodite and male gonadal 26G RNA and 22G RNA.

A) Percentage of antisense reads in hermaphrodite and male gonads classified as primary 26G RNA, secondary 22G RNA or other siRNAs type.

B) Normalized mean 26G RNA and 22G RNA reads in hermaphrodite and male gonads per gene.

Figure S3: Statistical analysis of gonadal mRNA and siRNA expression levels.

A) Mean normalized mRNA reads [54] and siRNAs in percentiles in hermaphrodite and male gonads. For 20 bins (each representing 5% of

bioRxiv preprint doi: https://doi.org/10.1101/398784; this version posted August 23, 2018. The copyright holder for this preprint (which was not certified by peer review) is the author/funder, who has granted bioRxiv a license to display the preprint in perpetuity. It is made available under aCC-BY-NC-ND 4.0 International license.

804 data i.e. 427 genes per bin in hermaphrodites and 504 in males) a
805 linear model was fitted (black line)
806 B) p-values indicate whether the linear model deviates from zero. The
807 most significant negative correlation between the levels of 22G RNA
808 and mRNA was found for the 5% of the genes with highest level of 22G
809 RNA expression (shaded).
810
811 **Figure S4:** Sex-differences in RNAi efficacy in female germlines.
812 Mean primary and secondary siRNA reads normalized to total reads in
813 gonads from hermaphrodites (circles indicate replicates n=4; data from
814 figure 3B) and *fog-3* males (n=2) raised on *gfp(RNAi)*. Mean secondary
815 siRNA/ primary siRNA ratio. T-test was applied for significance test; * =
816 $p<0.05$, *** = $p<0.001$.
817
818 **Additional file 2.xls:** Summary gonadal small RNA expression.
819 Analyses of sex-biased miRNA, piRNA, germline siRNA, sense and
820 antisense reads
821
822 **Additional file 3.xls:** Sequencing details.
823 Accession and genotype of each replicate
824
825
826

bioRxiv preprint doi: https://doi.org/10.1101/398784; this version posted August 23, 2018. The copyright holder for this preprint (which was not certified by peer review) is the author/funder, who has granted bioRxiv a license to display the preprint in perpetuity. It is made available under aCC-BY-NC-ND 4.0 International license.

827 **REFERENCES**

828 1. Miska EA, Ferguson-Smith AC. Transgenerational inheritance: Models and
829 mechanisms of non-DNA sequence-based inheritance. Science (80-.). 2016.
830 p. 59–63.
831 2. Grishok A, Tabara H, Mello CC. Genetic requirements for inheritance of
832 RNAi in *C. elegans*. Science. 2000;287:2494–7.
833 3. Luteijn MJ, van Bergeijk P, Kaaij LJT, Almeida MV, Roovers EF, Berezikov
834 E, et al. Extremely stable Piwi-induced gene silencing in *Caenorhabditis*
835 *elegans*. EMBO J. 2012;31:3422–30.
836 4. Shirayama M, Seth M, Lee HC, Gu W, Ishidate T, Conte D, et al. PiRNAs
837 initiate an epigenetic memory of nonself RNA in the *C. elegans* germline. Cell.
838 2012;150:65–77.
839 5. Schott D, Yanai I, Hunter CP. Natural RNA interference directs a heritable
840 response to the environment. Sci Rep. 2014;4:7387.
841 6. Fire A, Xu S, Montgomery MK, Kostas SA, Driver SE, Mello CC. Potent and
842 specific genetic interference by double-stranded RNA in *Caenorhabditis*
843 *elegans*. Nature. 1998;391:806–11.
844 7. Rechavi O, Minevich G, Hobert O. Transgenerational Inheritance of an
845 Acquired Small RNA-Based Antiviral Response in *C. elegans*. Cell.
846 2011;147:1248–56.
847 8. Jobson MA, Jordan JM, Sandrof MA, Hibshman JD, Lennox AL, Baugh LR.
848 Transgenerational Effects of Early Life Starvation on Growth, Reproduction,
849 and Stress Resistance in *Caenorhabditis elegans*. Genetics. 2015;201:201–
850 12.
851 9. Vastenhouw NL, Brunschwig K, Okihara KL, Muller F, Tijsterman M,

bioRxiv preprint doi: https://doi.org/10.1101/398784; this version posted August 23, 2018. The copyright holder for this preprint (which was not certified by peer review) is the author/funder, who has granted bioRxiv a license to display the preprint in perpetuity. It is made available under aCC-BY-NC-ND 4.0 International license.

852 Plasterk RHA. Gene expression: long-term gene silencing by RNAi. Nature.
853 2006;442:882.
854 10. Alcazar RM, Lin R, Fire AZ. Transmission dynamics of heritable silencing
855 induced by double-stranded RNA in *Caenorhabditis elegans*. Genetics.
856 2008;180:1275–88.
857 11. Lev I, Seroussi U, Gingold H, Bril R, Anava S, Rechavi O. MET-2-
858 Dependent H3K9 Methylation Suppresses Transgenerational Small RNA
859 Inheritance. Curr Biol. 2017;27:1138–47.
860 12. Winston WM, Molodowitch C, Hunter CP. Systemic RNAi in *C. elegans*
861 requires the putative transmembrane protein SID-1. Science. 2002;295:2456–
862 9.
863 13. Winston WM, Sutherlin M, Wright AJ, Feinberg EH, Hunter CP.
864 *Caenorhabditis elegans* SID-2 is required for environmental RNA interference.
865 Proc Natl Acad Sci. 2007;104:10565–70.
866 14. Tabara H, Yigit E, Siomi H, Mello CC. The dsRNA binding protein RDE-4
867 interacts with RDE-1, DCR-1, and a DExH-box helicase to direct RNAi in *C.*
868 *elegans*. Cell. 2002;109:861–71.
869 15. Parker GS, Eckert DM, Bass BL. RDE-4 preferentially binds long dsRNA
870 and its dimerization is necessary for cleavage of dsRNA to siRNA. RNA.
871 2006;12:807–18.
872 16. Sijen T, Fleenor J, Simmer F, Thijssen KL, Parrish S, Timmons L, et al.
873 On the Role of RNA Amplification in dsRNA-Triggered Gene Silencing. Cell.
874 2001;107:465–76.
875 17. Sijen T, Steiner FA, Thijssen KL, Plasterk RHA. Secondary siRNAs Result
876 from Unprimed RNA Synthesis and Form a Distinct Class. Science.

bioRxiv preprint doi: https://doi.org/10.1101/398784; this version posted August 23, 2018. The copyright holder for this preprint (which was not certified by peer review) is the author/funder, who has granted bioRxiv a license to display the preprint in perpetuity. It is made available under aCC-BY-NC-ND 4.0 International license.

877 2007;315:244–7.

878 18. Pak J, Fire A. Distinct Populations of Primary and Secondary Effectors

879 During RNAi in *C. elegans*. Science. 2007;315:241–4.

880 19. Gu W, Shirayama M, Conte D, Vasale J, Batista PJ, Claycomb JM, et al.

881 Distinct Argonaute-Mediated 22G-RNA Pathways Direct Genome Surveillance

882 in the *C. elegans* Germline. Mol Cell. 2009;36:231–44.

883 20. Grishok A, Sinskey JL, Sharp PA. Transcriptional silencing of a transgene

884 by RNAi in the soma of *C. elegans*. Genes Dev. 2005;19:683–96.

885 21. Guang S, Bochner AF, Burkhart KB, Burton N, Pavelec DM, Kennedy S.

886 Small regulatory RNAs inhibit RNA polymerase II during the elongation phase

887 of transcription. Nature. 2010;465:1097–101.

888 22. Buckley BA, Burkhart KB, Gu SG, Spracklin G, Kershner A, Fritz H, et al.

889 A nuclear Argonaute promotes multigenerational epigenetic inheritance and

890 germline immortality. Nature. 2012;489:447–51.

891 23. Martinez NJ, Ow MC, Reece-Hoyes JS, Barrasa MI, Ambros VR, Walhout

892 AJM. Genome-scale spatiotemporal analysis of *Caenorhabditis elegans*

893 microRNA promoter activity. Genome Res. 2008;18:2005–15.

894 24. Kato M, de Lencastre A, Pincus Z, Slack FJ. Dynamic expression of small

895 non-coding RNAs, including novel microRNAs and piRNAs/21U-RNAs, during

896 *Caenorhabditis elegans* development. Genome Biol. 2009;10:R54.

897 25. Alberti C, Manzenreither RA, Sowemimo I, Burkard TR, Wang J,

898 Mahofsky K, et al. Cell-Type specific sequencing of microRNAs from complex

899 animal tissues. Nat Methods. 2018;15:283–9.

900 26. Diag A, Schilling M, Klironomos F, Ayoub S, Rajewsky N. Regulation of

901 spatial and temporal gene expression in an animal germline. bioRxiv. Cold

bioRxiv preprint doi: https://doi.org/10.1101/398784; this version posted August 23, 2018. The copyright holder for this preprint (which was not certified by peer review) is the author/funder, who has granted bioRxiv a license to display the preprint in perpetuity. It is made available under aCC-BY-NC-ND 4.0 International license.

902 Spring Harbor Laboratory; 2018;348425.

903 27. Alvarez-Saavedra E, Horvitz HR. Many Families of *C. elegans* MicroRNAs

904 Are Not Essential for Development or Viability. Curr Biol. 2010;20:367–73.

905 28. McJunkin K, Ambros V. The embryonic mir-35 family of microRNAs

906 promotes multiple aspects of fecundity in *Caenorhabditis elegans*. G3.

907 2014;4:1747–54.

908 29. McEwen TJ, Yao Q, Yun S, Lee C-Y, Bennett KL. Small RNA in situ

909 hybridization in *Caenorhabditis elegans*, combined with RNA-seq, identifies

910 germline-enriched microRNAs. Dev Biol. 2016;418:248–57.

911 30. Han T, Manoharan AP, Harkins TT, Bouffard P, Fitzpatrick C, Chu DS, et

912 al. 26G endo-siRNAs regulate spermatogenic and zygotic gene expression in

913 *Caenorhabditis elegans*. Proc Natl Acad Sci U S A. 2009;106:18674–9.

914 31. Vasale JJ, Gu W, Thivierge C, Batista PJ, Claycomb JM, Youngman EM,

915 et al. Sequential rounds of RNA-dependent RNA transcription drive

916 endogenous small-RNA biogenesis in the ERGO-1/Argonaute pathway. Proc

917 Natl Acad Sci U S A. 2010;107:3582–7.

918 32. Conine CC, Batista PJ, Gu W, Claycomb JM, Chaves DA, Shirayama M,

919 et al. Argonautes ALG-3 and ALG-4 are required for spermatogenesis-specific

920 26G-RNAs and thermotolerant sperm in *Caenorhabditis elegans*. Proc Natl

921 Acad Sci U S A. 2010;107:3588–93.

922 33. Conine CC, Moresco JJ, Gu W, Shirayama M, Conte D, Yates JR, et al.

923 Argonautes Promote Male Fertility and Provide a Paternal Memory of

924 Germline Gene Expression in *C. elegans*. Cell. 2013;155:1532–44.

925 34. Gerson-Gurwitz A, Wang S, Sathe S, Green R, Yeo GW, Oegema K, et al.

926 A Small RNA-Catalytic Argonaute Pathway Tunes Germline Transcript Levels

bioRxiv preprint doi: https://doi.org/10.1101/398784; this version posted August 23, 2018. The copyright holder for this preprint (which was not certified by peer review) is the author/funder, who has granted bioRxiv a license to display the preprint in perpetuity. It is made available under aCC-BY-NC-ND 4.0 International license.

927 to Ensure Embryonic Divisions. Cell. 2016;165:396–409.
928 35. Wang G, Reinke V. A *C. elegans* Piwi, PRG-1, Regulates 21U-RNAs
929 during Spermatogenesis. Curr Biol. 2008;18:861–7.
930 36. Batista PJ, Ruby JG, Claycomb JM, Chiang R, Fahlgren N, Kasschau KD,
931 et al. PRG-1 and 21U-RNAs Interact to Form the piRNA Complex Required
932 for Fertility in *C. elegans*. Mol Cell. 2008;31:67–78.
933 37. Shi Z, Montgomery TA, Qi Y, Ruvkun G. High-throughput sequencing
934 reveals extraordinary fluidity of miRNA, piRNA, and siRNA pathways in
935 nematodes. Genome Res. 2013;23:497–508.
936 38. Das PP, Bagijn MP, Goldstein LD, Woolford JR, Lehrbach NJ,
937 Sapetschnig A, et al. Piwi and piRNAs Act Upstream of an Endogenous
938 siRNA Pathway to Suppress Tc3 Transposon Mobility in the *Caenorhabditis*
939 *elegans* Germline. Mol Cell. 2008;31:79–90.
940 39. Gu W, Lee HC, Chaves D, Youngman EM, Pazour GJ, Conte D, et al.
941 CapSeq and CIP-TAP identify pol ii start sites and reveal capped small RNAs
942 as *C. elegans* piRNA precursors. Cell. 2012;151:1488–500.
943 40. Killian DJ, Hubbard EJA. *Caenorhabditis elegans* germline patterning
944 requires coordinated development of the somatic gonadal sheath and the
945 germ line. Dev Biol. 2005;279:322–35.
946 41. Bukhari SIA, Vasquez-Rifo A, Gagné D, Paquet ER, Zetka M, Robert C, et
947 al. The microRNA pathway controls germ cell proliferation and differentiation
948 in *C. elegans*. Cell Res. 2012;22:1034–45.
949 42. Rios C, Warren D, Olson B, Abbott AL. Functional analysis of microRNA
950 pathway genes in the somatic gonad and germ cells during ovulation in *C.*
951 *elegans*. Dev Biol. 2017;426:115–25.

bioRxiv preprint doi: https://doi.org/10.1101/398784; this version posted August 23, 2018. The copyright holder for this preprint (which was not certified by peer review) is the author/funder, who has granted bioRxiv a license to display the preprint in perpetuity. It is made available under aCC-BY-NC-ND 4.0 International license.

952 43. Fraser AG, Kamath RS, Zipperlen P, Martinez-Campos M, Sohrmann M,
953 Ahringer J. Functional genomic analysis of *C. elegans* chromosome I by
954 systematic RNA interference. Nature. 2000;408:325–30.
955 44. Gönczy P, Echeverri C, Oegema K, Coulson A, Jones SJ, Copley RR, et
956 al. Functional genomic analysis of cell division in *C. elegans* using RNAi of
957 genes on chromosome III. Nature. 2000;408:331–6.
958 45. Green RA, Kao H-L, Audhya A, Arur S, Mayers JR, Fridolfsson HN, et al.
959 A High-Resolution *C. elegans* Essential Gene Network Based on Phenotypic
960 Profiling of a Complex Tissue. Cell. 2011;145:470–82.
961 46. Reinke V, Gil IS, Ward S, Kazmer K. Genome-wide germline-enriched and
962 sex-biased expression profiles in *Caenorhabditis elegans*. Development.
963 2003;131:311–23.
964 47. Roovers EF, Rosenkranz D, Mahdipour M, Han C-T, He N,
965 Chuva de Sousa Lopes SM, et al. Piwi Proteins and piRNAs in Mammalian
966 Oocytes and Early Embryos. Cell Rep. 2015;10:2069–82.
967 48. Ma X, Zhu Y, Li C, Xue P, Zhao Y, Chen S, et al. Characterisation of
968 *Caenorhabditis elegans* sperm transcriptome and proteome. BMC Genomics.
969 2014;15:168.
970 49. Ellis RE, Kimble J. The fog-3 gene and Regulation of Cell Fate in the
971 Germ line of *Caenorhabditis elegans*. Genetics. 1995;139:561–77.
972 50. Noble DC, Aoki ST, Ortiz MA, Kim KW, Verheyden JM, Kimble J.
973 Genomic Analyses of Sperm Fate Regulator Targets Reveal a Common Set
974 of Oogenic mRNAs in *Caenorhabditis elegans*. Genetics. 2016;202:221–34.
975 51. Ruby JG, Jan C, Player C, Axtell MJ, Lee W, Nusbaum C, et al. Large-
976 Scale Sequencing Reveals 21U-RNAs and Additional MicroRNAs and

bioRxiv preprint doi: https://doi.org/10.1101/398784; this version posted August 23, 2018. The copyright holder for this preprint (which was not certified by peer review) is the author/funder, who has granted bioRxiv a license to display the preprint in perpetuity. It is made available under aCC-BY-NC-ND 4.0 International license.

977 Endogenous siRNAs in *C. elegans*. Cell. 2006;127:1193–207.
978 52. Billi AC, Freeberg MA, Day AM, Chun SY, Khivansara V, Kim JK. A
979 conserved upstream motif orchestrates autonomous, germline-enriched
980 expression of *Caenorhabditis elegans* piRNAs. Copenhaver GP, editor. PLoS
981 Genet. 2013;9:e1003392.
982 53. Yang W, Dierking K, Schulenburg H. WormExp: a web-based application
983 for a *Caenorhabditis elegans* -specific gene expression enrichment analysis.
984 Bioinformatics. 2016;32:943–5.
985 54. West SM, Mecenas D, Gutwein M, Aristizábal-Corrales D, Piano F,
986 Gunsalus KC. Developmental dynamics of gene expression and alternative
987 polyadenylation in the *Caenorhabditis elegans* germline. Genome Biol.
988 2018;19:8.
989 55. Bagijn MP, Goldstein LD, Sapetschnig A, Weick E-M, Bouasker S,
990 Lehrbach NJ, et al. Function, targets, and evolution of *Caenorhabditis elegans*
991 piRNAs. Science. 2012;337:574–8.
992 56. Chen F, Hersh BM, Conradt B, Zhou Z, Riemer D, Gruenbaum Y, et al.
993 Translocation of *C. elegans* CED-4 to nuclear membranes during
994 programmed cell death. Science. 2000;287:1485–9.
995 57. Luitjens C, Gallegos M, Kraemer B, Kimble J, Wickens M. CPEB proteins
996 control two key steps in spermatogenesis in *C. elegans*. Genes Dev.
997 2000;14:2596–609.
998 58. Sumiyoshi E, Sugimoto A, Yamamoto M. Protein phosphatase 4 is
999 required for centrosome maturation in mitosis and sperm meiosis in *C.*
1000 *elegans*. J Cell Sci. 2002;115:1403–10.
1001 59. Zhu G, Salazar G, Zlatic SA, Fiza B, Doucette MM, Heilman CJ, et al.

bioRxiv preprint doi: https://doi.org/10.1101/398784; this version posted August 23, 2018. The copyright holder for this preprint (which was not certified by peer review) is the author/funder, who has granted bioRxiv a license to display the preprint in perpetuity. It is made available under aCC-BY-NC-ND 4.0 International license.

1002 SPE-39 family proteins interact with the HOPS complex and function in
1003 lysosomal delivery. Mol Biol Cell. 2009;20:1223–40.
1004 60. von Tobel L, Mikeladze-Dvali T, Delattre M, Balestra FR, Blanchoud S,
1005 Finger S, et al. SAS-1 Is a C2 Domain Protein Critical for Centriole Integrity in
1006 *C. elegans*. Dutcher SK, editor. PLoS Genet. 2014;10:e1004777.
1007 61. Kang C, You Y -j., Avery L. Dual roles of autophagy in the survival of
1008 *Caenorhabditis elegans* during starvation. Genes Dev. 2007;21:2161–71.
1009 62. Kalis AK, Kroetz MB, Larson KM, Zarkower D. Functional genomic
1010 identification of genes required for male gonadal differentiation in
1011 *Caenorhabditis elegans*. Genetics. 2010;185:523–35.
1012 63. Nelson MD, Zhou E, Kiontke K, Fradin H, Maldonado G, Martin D, et al. A
1013 bow-tie genetic architecture for morphogenesis suggested by a genome-wide
1014 RNAi screen in *Caenorhabditis elegans*. Chisholm AD, editor. PLoS Genet.
1015 2011;7:e1002010.
1016 64. Pak J, Maniar JM, Mello CC, Fire A. Protection from Feed-Forward
1017 Amplification in an Amplified RNAi Mechanism. Cell. 2012;151:885–99.
1018 65. Zhang C, Montgomery TA, Fischer SEJ, Garcia SMDA, Riedel CG,
1019 Fahlgren N, et al. The *Caenorhabditis elegans* RDE-10/RDE-11 Complex
1020 Regulates RNAi by Promoting Secondary siRNA Amplification. Curr Biol.
1021 2012;22:881–90.
1022 66. Tsai H-Y, Chen C-CG, Conte D, Moresco JJ, Chaves DA, Mitani S, et al.
1023 A Ribonuclease Coordinates siRNA Amplification and mRNA Cleavage during
1024 RNAi. Cell. 2015;160:407–19.
1025 67. Ooi SL, Priess JR, Henikoff S. Histone H3.3 Variant Dynamics in the
1026 Germline of *Caenorhabditis elegans*. PLoS Genet. 2006;2:e97.

bioRxiv preprint doi: https://doi.org/10.1101/398784; this version posted August 23, 2018. The copyright holder for this preprint (which was not certified by peer review) is the author/funder, who has granted bioRxiv a license to display the preprint in perpetuity. It is made available under aCC-BY-NC-ND 4.0 International license.

1027 68. Barton MK, Schedl TB, Kimble J. Gain-of-Function Mutations of fem-3, a
1028 Sex-Determination Gene in *Caenorhabditis elegans*. Genetics. 1987;115.
1029 69. McJunkin K, Ambros V. A microRNA family exerts maternal control on sex
1030 determination in *C. elegans*. Genes Dev. 2017;31:422–37.
1031 70. Lim LP, Lau NC, Weinstein EG, Abdelhakim A, Yekta S, Rhoades MW, et
1032 al. The microRNAs of *Caenorhabditis elegans*. Genes Dev. 2003;17:991–
1033 1008.
1034 71. de Lencastre A, Pincus Z, Zhou K, Kato M, Lee SS, Slack FJ. MicroRNAs
1035 Both Promote and Antagonize Longevity in *C. elegans*. Curr Biol.
1036 2010;20:2159–68.
1037 72. Pincus Z, Smith-Vikos T, Slack FJ. MicroRNA Predictors of Longevity in
1038 *Caenorhabditis elegans*. Kim SK, editor. PLoS Genet. 2011;7:e1002306.
1039 73. Ortiz MA, Noble D, Sorokin EP, Kimble J. A new dataset of spermatogenic
1040 vs. oogenic transcriptomes in the nematode *Caenorhabditis elegans*. G3.
1041 2014;4:1765–72.
1042 74. van Wolfswinkel JC, Claycomb JM, Batista PJ, Mello CC, Berezikov E,
1043 Ketting RF. CDE-1 Affects Chromosome Segregation through Uridylation of
1044 CSR-1-Bound siRNAs. Cell. 2009;139:135–48.
1045 75. Claycomb JM, Batista PJ, Pang KM, Gu W, Vasale JJ, van Wolfswinkel
1046 JC, et al. The Argonaute CSR-1 and Its 22G-RNA Cofactors Are Required for
1047 Holocentric Chromosome Segregation. Cell. 2009;139:123–34.
1048 76. Yigit E, Batista PJ, Bei Y, Pang KM, Chen C-CG, Tolia NH, et al. Analysis
1049 of the *C. elegans* Argonaute Family Reveals that Distinct Argonautes Act
1050 Sequentially during RNAi. Cell. 2006;127:747–57.
1051 77. Hodgkin J, Horvitz HR, Brenner S. Nondisjunction Mutants of the

bioRxiv preprint doi: https://doi.org/10.1101/398784; this version posted August 23, 2018. The copyright holder for this preprint (which was not certified by peer review) is the author/funder, who has granted bioRxiv a license to display the preprint in perpetuity. It is made available under aCC-BY-NC-ND 4.0 International license.

1052 Nematode *Caenorhabditis elegans*. Genetics. 1979;91:67–94.

1053 78. Zhang C, Montgomery TA, Gabel HW, Fischer SEJ, Phillips CM, Fahlgren

1054 N, et al. mut-16 and other mutator class genes modulate 22G and 26G siRNA

1055 pathways in *Caenorhabditis elegans*. Proc Natl Acad Sci U S A.

1056 2011;108:1201–8.

1057 79. Kamath RS, Martinez-Campos M, Zipperlen P, Fraser AG, Ahringer J.

1058 Effectiveness of specific RNA-mediated interference through ingested double-

1059 stranded RNA in *Caenorhabditis elegans*. Genome Biol.

1060 2001;2:RESEARCH0002.

1061 80. O'Connell J, Arganda-Carreras I, Frise E, Kaynig V, Longair M, Pietzsch

1062 T, et al. Fiji: an open-source platform for biological-image analysis. Nat

1063 Methods. 2012;9:676–82.

1064 81. Peters N, Perez DE, Song MH, Liu Y, Muller-Reichert T, Caron C, et al.

1065 Control of mitotic and meiotic centriole duplication by the Plk4-related kinase

1066 ZYG-1. J Cell Sci. 2010;123:795–805.

1067

1068

1069

1070

1071

bioRxiv preprint doi: https://doi.org/10.1101/398784; this version posted August 23, 2018. The copyright holder for this preprint (which was not certified by peer review) is the author/funder, who has granted bioRxiv a license to display the preprint in perpetuity. It is made available under aCC-BY-NC-ND 4.0 International license.

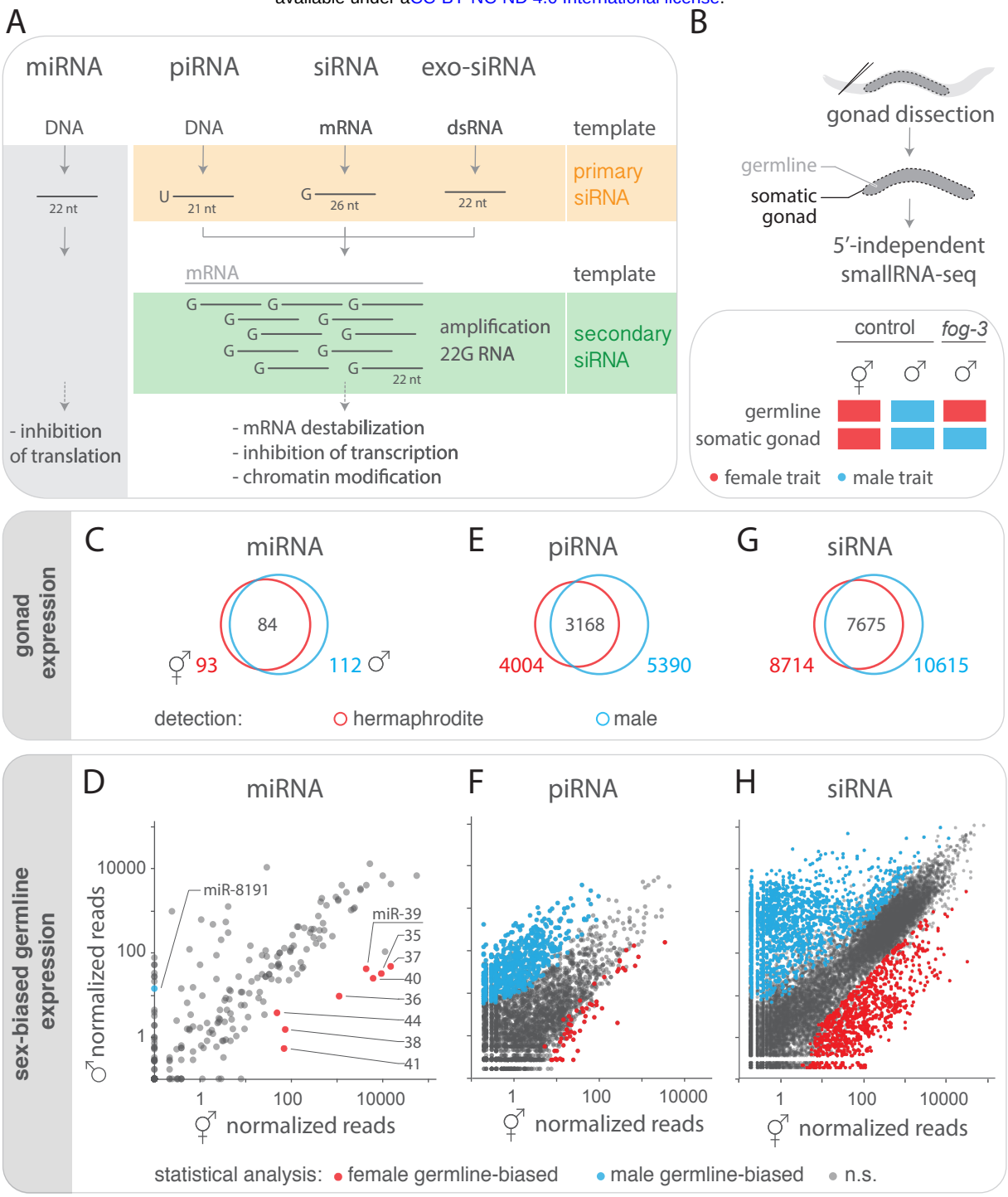

Figure 1

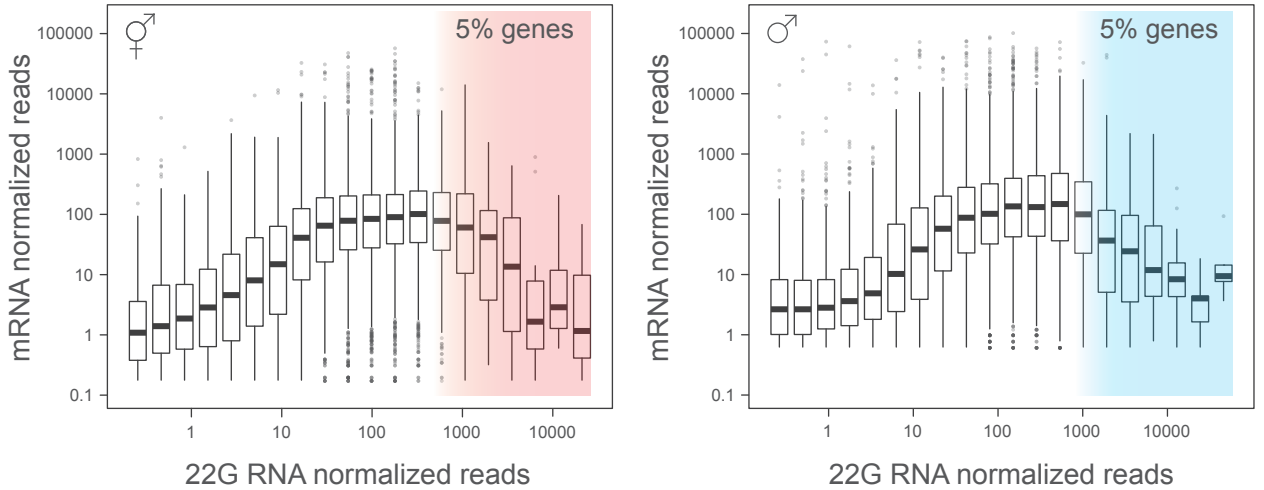
♀
5% genes
mRNA normalized reads
100000
10000
1000
100
10
1
0.1
1
10
100
1000
10000
22G RNA normalized reads
♂
5% genes
mRNA normalized reads
100000
10000
1000
100
10
1
0.1
1
10
100
1000
10000
22G RNA normalized reads

Figure 2

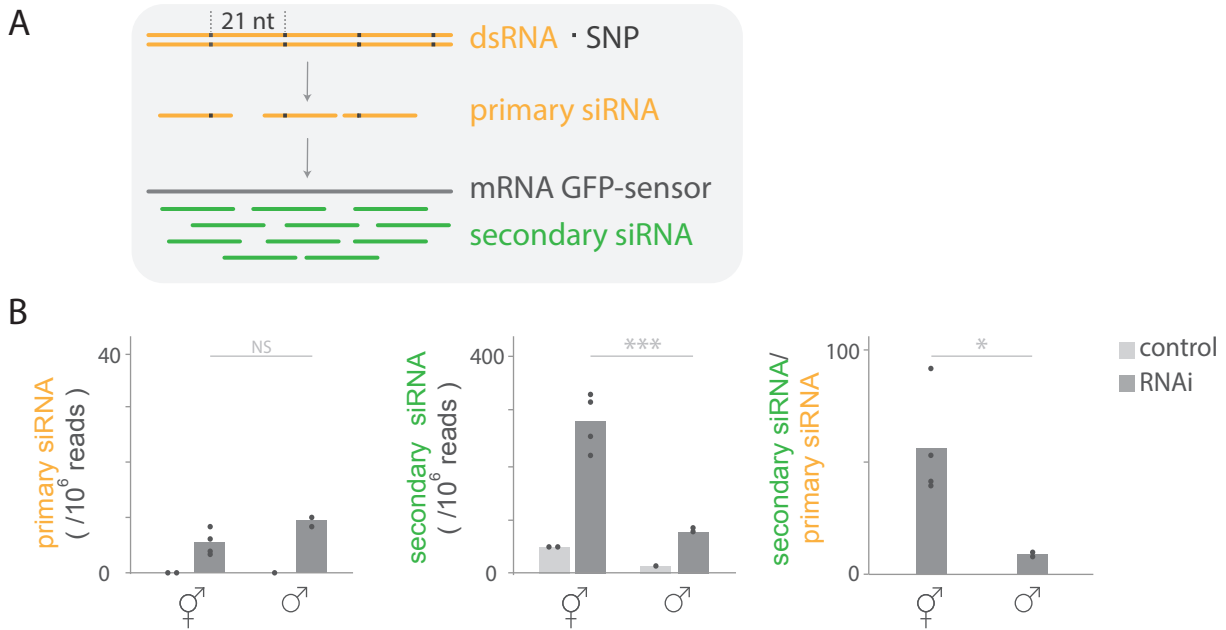
A
21 nt
dsRNA · SNP
primary siRNA
mRNA GFP-sensor
secondary siRNA
B
primary siRNA
(/10^6 reads)
40
0
NS
secondary siRNA
(/10^6 reads)
400
0
***
secondary siRNA/
primary siRNA
100
0
*
control
RNAi

Figure 3

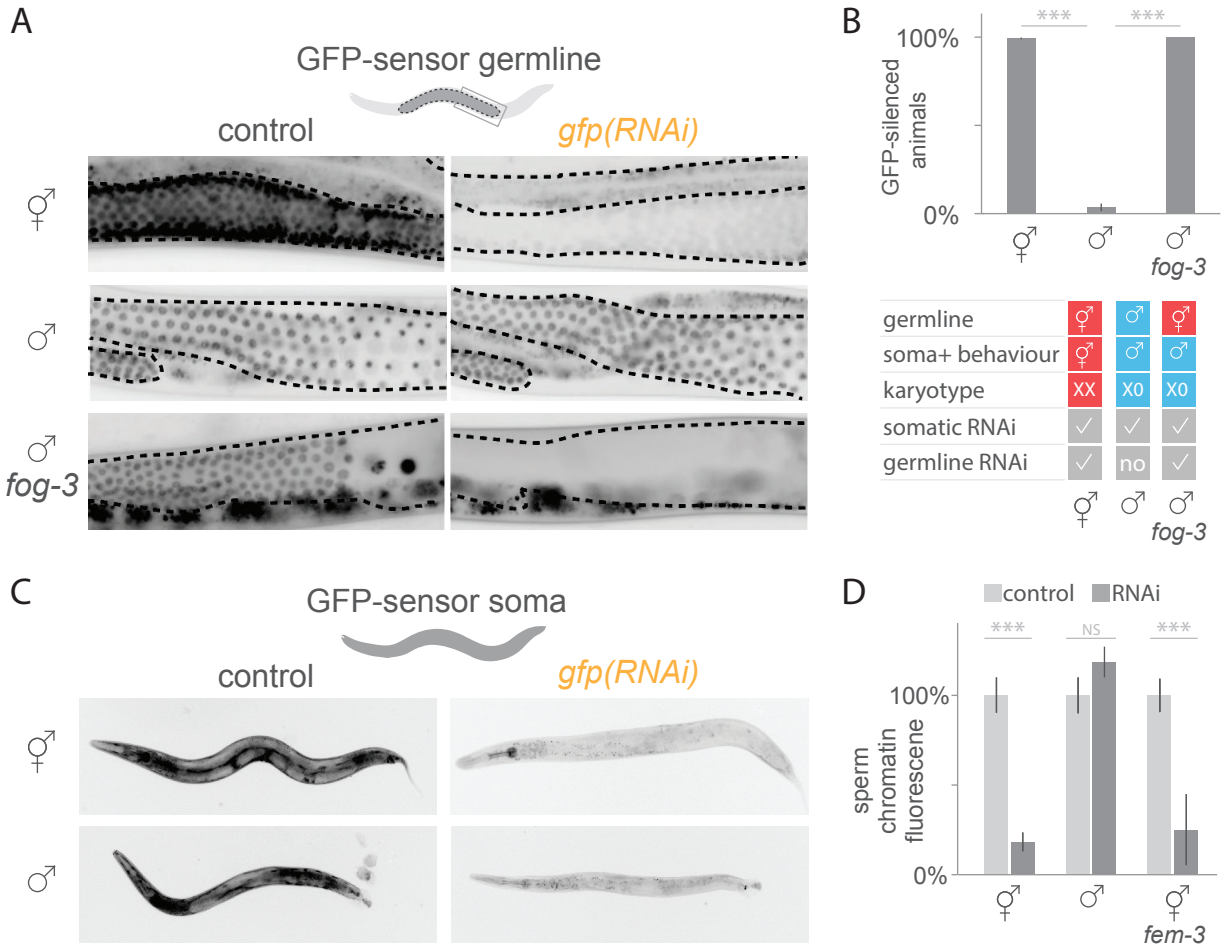
A
GFP-sensor germline
control
gfp(RNAi)
fog-3
B
GFP-silenced animals
100%
0%
***
***
fog-3
germline
soma+ behaviour
karyotype
somatic RNAi
germline RNAi
XX
X0
X0
no
fog-3
C
GFP-sensor soma
control
gfp(RNAi)
D
control
RNAi
sperm chromatin fluorescene
100%
0%
***
NS
***
fem-3

Figure 4

bioRxiv preprint doi: https://doi.org/10.1101/398784; this version posted August 23, 2018. The copyright holder for this preprint (which was not certified by peer review) is the author/funder, who has granted bioRxiv a license to display the preprint in perpetuity. It is made available under aCC-BY-NC-ND 4.0 International license.

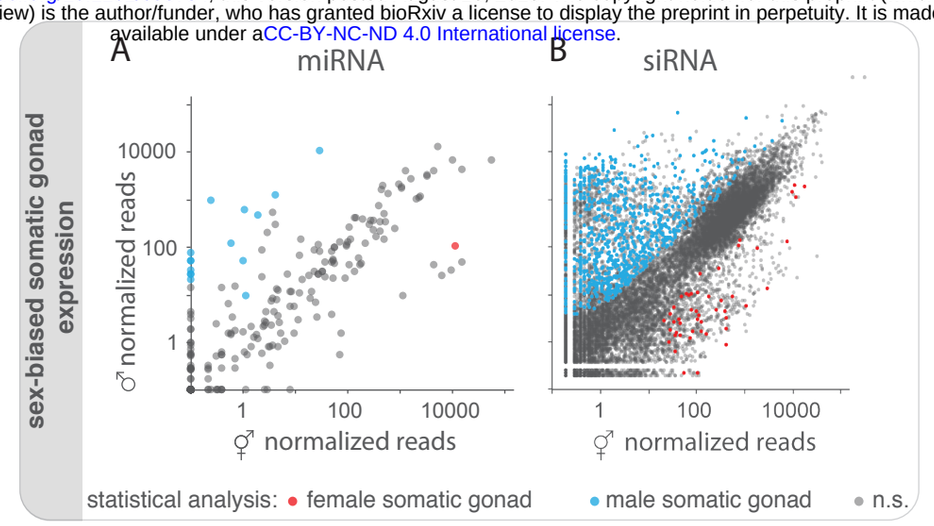

Figure S1

bioRxiv preprint doi: https://doi.org/10.1101/398784; this version posted August 23, 2018. The copyright holder for this preprint (which was not certified by peer review) is the author/funder, who has granted bioRxiv a license to display the preprint in perpetuity. It is made available under aCC-BY-NC-ND 4.0 International license.

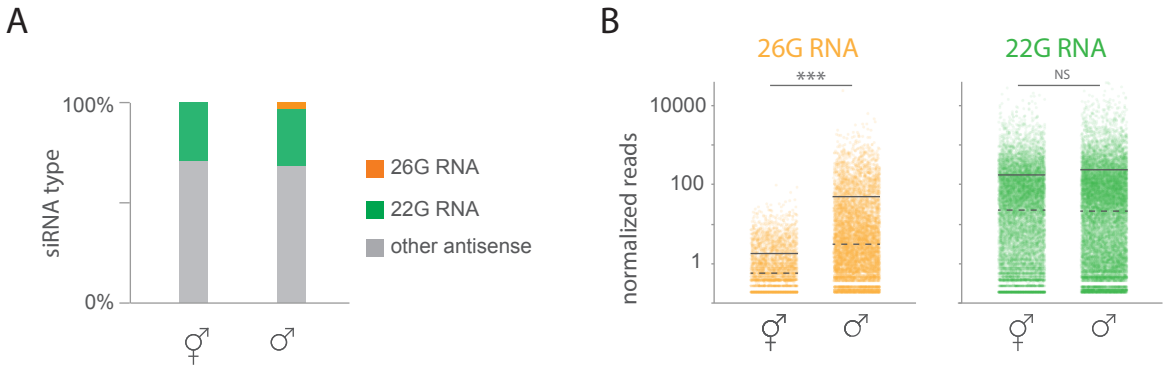

Figure S2

bioRxiv preprint doi: https://doi.org/10.1101/398784; this version posted August 23, 2018. The copyright holder for this preprint (which was not certified by peer review) is the author/funder, who has granted bioRxiv a license to display the preprint in perpetuity. It is made available under aCC-BY-NC-ND 4.0 International license.

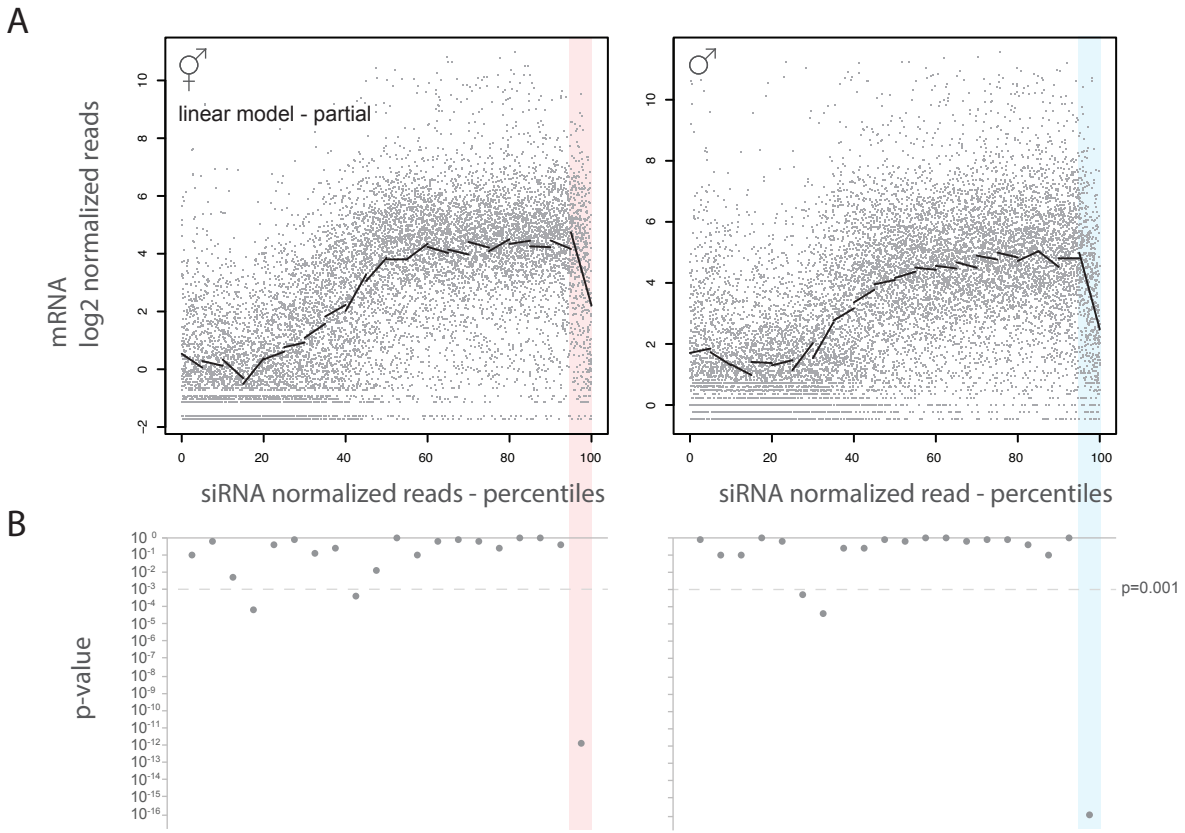

Figure S3

bioRxiv preprint doi: https://doi.org/10.1101/398784; this version posted August 23, 2018. The copyright holder for this preprint (which was not certified by peer review) is the author/funder, who has granted bioRxiv a license to display the preprint in perpetuity. It is made available under aCC-BY-NC-ND 4.0 International license.

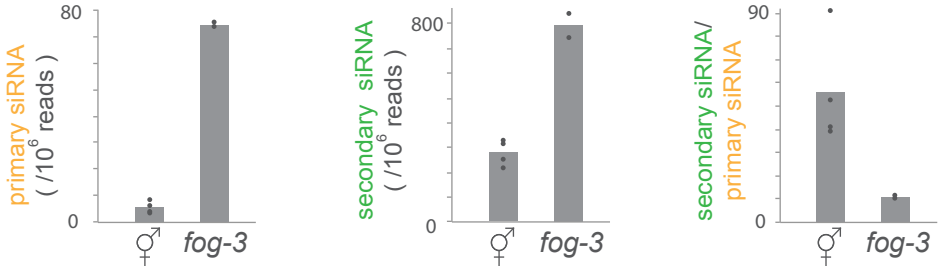

Figure S4